Heliyon 10 (2024) e37838

Contents lists available at ScienceDirect

Heliyon

journal homepage: www.cell.com/heliyon

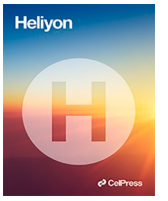

Research article

Progression from cardiomyopathy to heart failure with reduced ejection fraction: A CORIN deficient course

Jun-yan Kan [1], Dong-chen Wang [1], Zi-hao Jiang [1], Li-da Wu, Ke Xu, Yue Gu [*]

Division of Cardiology, Nanjing First Hospital, Nanjing Medical University, Nanjing, China

ARTICLE INFO

Keywords:
Cardiomyopathy
Molecular subtypes
Bioinformatics
Heart failure with reduced ejection fraction
CORIN

ABSTRACT

Cardiomyopathies, encompassing hypertrophic cardiomyopathy (HCM) and dilated cardiomyopathy (DCM), constitute a diverse spectrum of heart muscle diseases that often culminating in heart failure (HF). The inherent molecular heterogeneity of these conditions has implications for prognosis and therapeutic strategies.

Publicly available microarray and RNA sequencing (RNA-seq) data sets of HCM (n = 106 from GSE36961) and DCM (n = 18 from GSE135055 and 166 from GSE141910) patients were employed for our analysis. The Non-negative Matrix Factorization (NMF) algorithm was applied to explore the molecular stratification within HCM and DCM, and enrichment analysis was performed to delineate their biological characteristics. By integrating bulk and single-nucleus RNA-seq (snRNA-seq) data, we identified a potential biomarker for HCM progression and cardiac fibrosis, which was subsequently validated using mendelian randomization and in vitro.

Our application of NMF identified two distinct molecular clusters. Particularly, a profibrotic, heart failure with reduced ejection fraction (HFrEF)-resembling Cluster 1 emerged, characterized by diminished expression of CORIN and a high degree of fibroblast activation. This cluster also exhibited lower left ventricular ejection fraction (LVEF) and worse prognostic outcomes, establishing the significance of this molecular subclassification. We further found that overexpression of CORIN could mitigate TGFβ1-induced expression of col1a1 and α-SMA in neonatal rat cardiac fibroblasts.

Our results indicated the heterogeneity of HCM population, and further evidenced the participation of corin in the progression of HCM, DCM and HFrEF. Nevertheless, our study is constrained by the lack of corresponding clinical data and experimental validation of the identified subtypes. Therefore, further studies are warranted to elucidate the downstream pathways of corin and to validate these findings in independent patient cohorts.

1. Background

Hypertrophic cardiomyopathy (HCM) and dilated cardiomyopathy (DCM) are two prevalent forms of cardiomyopathy, each associated with a relatively high morbidity and mortality. HCM is typically manifested by an asymmetrical left ventricular

* Corresponding author. Department of Cardiology, Nanjing First Hospital Affiliated to Nanjing Medical University, No. 68 Changle Road, Nanjing 210006, China.

E-mail addresses: kanjy98@126.com (J.-y. Kan), wdcmed1995@163.com (D.-c. Wang), jiangzihao357@163.com (Z.-h. Jiang), lidawunjmu@outlook.com (L.-d. Wu), xukehigh123@stu.njmu.edu.cn (K. Xu), guyue_jessica@163.com (Y. Gu).

[1] These authors contributed equally to this work and share first authorship.

https://doi.org/10.1016/j.heliyon.2024.e37838
Received 8 January 2024; Received in revised form 9 September 2024; Accepted 11 September 2024
Available online 11 September 2024

hypertrophy, which cannot be explained by any other cardiac or systemic disease [1]. In contrast, DCM is distinguished by dilation of the left ventricle. Both HCM and DCM may lead to subsequent contractile dysfunction [2].

Regarding their etiology, HCM is primarily a heritable cardiovascular disease deriving from the pathogenic mutation of genes associated with myofilaments, with a minority of cases remaining idiopathic [3]. This condition affects approximately 1 in 500 adults [4]. In comparison, DCM presents a more complex etiology, with heterogeneous causes, and an estimated prevalence of 1:250 to 500 [5]. Notwithstanding the strides made in genetics and epidemiology offering up-to-date insights into the pathogenesis of these forms of cardiomyopathy, the precise molecular mechanisms driving the development and progression of these conditions continue to be not fully comprehended.

Heart failure (HF) with reduced ejection fraction (HFrEF) represents the terminal stage of both HCM and DCM, characterized by diminished cardiac output and the emergence of consequent clinical symptoms such as dyspnea, fatigue, and fluid retention. HFrEF, defined by a left ventricular ejection fraction (LVEF) of 40 % or less, is marked by progressive left ventricular dilatation and adverse cardiac remodeling [6].

In spite of significant advancements in medical therapy, including the application of angiotensin receptor-neprilysin inhibitors, beta-blockers, SGLT2 inhibitors and mineralocorticoid receptor antagonists, HFrEF continues to be a leading cause of morbidity and mortality globally [7]. As such, therapeutic strategies aimed at delaying and obstructing the progression of cardiomyopathy to HF hold promising potential.

Through the utilization of non-negative matrix factorization (NMF) and the integration of bulk RNA sequencing (RNA-seq) and single-nucleus RNA-seq (snRNA-seq) data, we identified a subset of cardiomyopathy patients that displayed a transcriptional profile associated with contractile dysfunction. This profile was characterized by down-regulation of CORIN, activation of fibroblasts and enhanced signaling of TGFβ, LAMININ and COLLAGEN. Intriguingly, our research indicated that the overexpression of CORIN might mitigate the TGF-$\beta 1$-mediated fibroblast activation and collagen synthesis. Our findings suggested the molecular heterogeneity of cardiomyopathy, and further evidenced the role of cardiac corin as modulator and marker of HCM, DCM and HFrEF.

2. Methods

2.1. Data collection and pre-process

The transcriptomic datasets used in this study were delineated in Supplementary Table S1. We incorporated microarray and bulk RNA-seq datasets from a HCM (GSE36961) and two DCM (GSE135055, GSE141910) cohorts to identify and verify cardiomyopathy subgroups [8,9]. For the recognition of phenotypes, we utilized bulk RNA-seq data drawn from the HFrEF and HFpEF cohorts, sourced from the Zenodo database [10]. Within the context of this study, HFrEF patients exhibiting an LVEF of less than 20 were classified as severe cases.

Subsequently, we integrated the results of bulk RNA-seq with two snRNA-seq datasets: GSE181764 and SCP1303 from Broad Institute's Single Cell Portal [11,12]. Corresponding demographics and prognosis data were collected from published articles and supplementary materials. To ascertain the association between the transcriptome and phenotype at molecular and cellular levels, we also collected bulk RNA-seq data of MYBPC3-mutated engineered cardiac tissues constructs (ECTs) and induced pluripotent stem cell derived cardiomyocytes along with TGF-β1 treated cardiac fibroblasts [13,14]. Datasets from the Gene Expression Omnibus (GEO) database were accessed using the "GEOquery" R package [15]. Following the acquisition, the gene expression matrix was log transformed and normalized with "normalizeBetweenArrays" function from the "limma" package [16].

2.2. Single-nucleus RNA sequencing data processing

A standard snRNA-seq data processing workflow was performed with the Seurat v4. Parameters for clustering and dimensionality reduction were defined, with cluster annotations made in reference to the corresponding descriptions in the source literature [17,18]. Owning to computational constraints, snRNA-seq data was down-sampled, allowing for 2000 cells from each cluster to be used in subsequent analyses. For sample clustering, pseudo-bulk expression matrixes were prepared by combining data from all cell types per donor.

2.3. Clinical characteristics

Clinical characteristics of sample donors, such as sex and age, were collected from the accessary phenotype data extracted from GEO datasets. Specifically, we acquired detailed baseline characteristics, medical history, imaging markers and survival time information of patients involved in GSE135055 from supplementary files [19]. Baseline characteristics were presented as medians and interquartile ranges, with exact tests applied for comparisons between cardiomyopathy clusters.

2.4. Non-negative matrix factorization

NMF is an unsupervised learning technique used to decompose an original matrix into a lower dimensional representation. For sample clustering, we utilized the "Muscle contraction-Cardiac conduction" gene set from the Reactome Knowledgebase database (https://reactome.org) [20]. The standard NMF algorithm, based on Kullback-Leibler divergence, was implemented on both HCM and DCM samples using the namesake package [21]. For snRNA-seq samples, NMF was performed on pseudo-bulk format data. The optimal

factorization rank, or cluster number, was determined by the cophenetic correlation coefficients.

2.5. Survival analysis

A total of 18 DCM patients from GSE135055, with entire survival time data, were employed for survival analysis. A multivariate Cox proportional hazards regression model was used to fit the time period from initial symptoms to heart transplantation. After accounting for factors such as RNA-seq quality, sex, age, smoking history, valvular disease, diabetes, pulmonary hypertension, atrial fibrillation, LVEF and fibrosis percentage, adjusted survival curves were visualized and compared between cardiomyopathy clusters using the log-rank test.

2.6. Differential expression analysis

In accordance with the NMF results, two cardiomyopathy clusters were identified. Differential expression analysis was conducted respectively between the HCM clusters and the control group using the "limma" package [16]. The criteria for differentially expressed genes (DEGs) were set as absolute log2 fold change (log2FC) > 1, in conjunction with an adjusted P-value <0.05. The Benjamini & Hochberg method was applied to control the false discover rate (FDR). DEGs were visualized as volcano plots and heatmaps. The shared DEGs, comparing the two HCM clusters with the control group separately, were identified and depicted in Venn plot.

Meanwhile, Kruskal-Wallis test was employed for multi-group comparison of specific genes. The correlation between DEGs and clinical characteristics was calculated using the "corrplot" package.

2.7. Gene set enrichment analysis

Gene set enrichment analysis (GSEA) is a computational method determining whether an a priori defined set of genes exhibits statistically significant concordance [22]. Genes were sorted for GSEA according to their expression fold change between HCM clusters. Then, the sorted genes were respectively enriched to Gene Ontology (GO) and Kyoto Encyclopedia of Genes and Genomes (KEGG) pathways using the "clusterProfiler" package [23,24]. The Benjamini & Hochberg method was employed for statistic adjustment, with $p < 0.05$ deemed as significant.

2.8. Weighted gene co-expression network analysis

The Weighted Gene Co-expression Network Analysis (WGCNA) was conducted to depict the correlation patterns among genes across samples. This method was performed on the gene expression matrix of 106 HCM samples using the "WGCNA" package [25]. We calculated the median absolute deviation of genes and incorporated 5000 genes with the largest values. The quality of samples was assessed, and no outliers were pruned. To select the proper soft threshold, we evaluated the scale independence and mean connectivity at different power levels. For equilibrium, 6 was picked as the optimal soft threshold. Additionally, we set the minimum gene module size at 50 and merged similar gene modules based on the correlation of their eigengenes. To associate gene modules with clinical traits, module-trait relationships were estimated according to Pearson correlation analysis and visualized as heatmap. For further functional insights, we conducted an enrichment analysis on gene modules with a statistically significant threshold set at $p < 0.05$ and $q < 0.05$.

2.9. ML methods for feature selection

In order to discern the hub genes between HCM clusters, three ML methods were implemented: random forest, support vector machines (SVM)-recursive feature elimination (RFE), and least absolute shrinkage and selection operator (LASSO) regression. We constructed a random forest model with 500 trees using the "randomForest" package. Feature importance was assessed based on the mean decrease in accuracy, and features with an importance exceeding 12 were retained. In the case of SVM-RFE method, we utilized the "rfe" function from the "caret" package, with radial basis functions serving as the SVM kernel. Furthermore, fivefold cross-validation was applied to derive the optimal hyperparameters of the SVM model. To eliminate superfluous features, we documented the least number of variables that provided the highest accuracy. As for LASSO regression, we randomly partitioned 70 % of samples into a training set and the remnant formed the test set. In the training set, we fitted the LASSO model using the "glmnet" package and calculated the coefficients of variables at different lambda values. For proper lambda selection, tenfold cross-validation was applied to estimate cross-validated errors with corresponding lambda values. We selected the lambda value that resulted in the minimum mean cross-validated error. The LASSO model, built based on the chosen lambda, was then tested using the test set. The intersection of hub genes identified by the aforementioned ML methods was visualized using an UpSet plot [26].

2.10. Evaluation of diagnostic capacity

Following feature selection, the identified hub genes were employed to differentiate HCM clusters. Generally, the expression levels of these genes in the control group and HCM clusters were visualized. The predictive efficacies were then evaluated by constructing receiver operating characteristic (ROC) curves. Single factor ROC curves were generated using the "pROC" package, and the areas under ROC curve (AUC) were calculated [27]. For multi-factor ROC curve construction, a binomial generalized linear model integrating the identified hub genes was fitted using the "ROCR" package [28].

2.11. Disease trajectory inference

Cardiomyopathy is acknowledged to potentially progress to heart failure. To categorize clusters, 8793 DEGs between HF with preserved ejection fraction (HFpEF) and control, along with 6802 DEGs between HFrEF and control, were derived from Virginia's study [29]. We sought to employ trajectory inference algorithm, typically used for pseudo-time analysis of cells, to predict the progression course of cardiomyopathy to HF. Based on the DEGs in HFpEF and HFrEF, the transcriptomic trajectory of healthy controls and cardiomyopathy patients were inferred using the "SCORPIUS" package. The inferred sample trajectory was thus considered as the progression course of cardiomyopathy.

2.12. Restricted cubic spline

LVEF is a key marker of the severity of HFrEF. The correlation between LVEF and CORIN expression was examined in both non-falling controls and HFrEF cases. Restricted cubic spline (RCS) was applied to model their non-linear correlations. Considering HFrEF cohort size ($n = 95$), 4 knots were taken in RCS fitting.

2.13. Cell fractions imputation

To investigate changes in the cell components of myocardial tissue in HCM, CIBERSORTx (https://cibersortx.stanford.edu/) was employed to estimate the abundance of heart cell subtypes [30]. CIBERSORTx is a deconvolution algorithm that predicts cell proportion in mixed samples. A signature matrix was prepared from the snRNA-seq dataset GSE181764, and finely-divided cell subtypes were merged. During the imputation process, the permutation test was performed 1000 times. The Wilcoxon signed-rank test was used to compare cell abundance between HCM clusters. Simultaneously, correlation coefficients between DEGs and myocardial cell types were calculated and those with a $p < 0.05$ were noted. In addition, trends in cell components were fitted based on the inferred trajectory with generalized additive model.

2.14. Differential abundance analysis

To verify the differences in the proportion of each cell type between cardiomyopathy clusters, we applied Milo algorithm with the "miloR" package [31]. The Milo algorithm models cellular states as overlapping neighborhoods on K-nearest neighbors graphs and tests for differential abundance. A weighted version of the Benjamini–Hochberg method was embedded into Milo to control spatial FDR. During Milo analysis, we constructed a KNN graph using the buildGraph function, considering 20 nearest neighbors and 30 dimensions. Then, we used makeNhoods function to construct neighborhood with default parameters. For visualization, neighborhoods with a spatial FDR <0.25 were deemed differentially abundant and color-marked. Neighborhood was further annotated to a cell type if more than 70 % of the cells in it belonged to that cell type; otherwise, the neighborhood was labelled as "mixed".

2.15. Scissor analysis

Scissor algorithm was employed to integrate bulk RNA-seq and snRNA-seq data, identifying phenotype-related cell types [32]. The Scissor function was performed on the snRNA-seq dataset SCP1303, respectively linked to HCM cohort (GSE36961) and DCM cohort (GSE135055) with parameters: alpha = 0.5, family = "binomial". Expression of identified hub genes were compared among Scissor-positive, Scissor-negative and background cells. Cardiomyopathy subtype-related cells were gathered for further analyses.

2.16. Cell-cell interaction analyses

Alterations in cell-cell interaction between cardiomyopathy subtype-related cells were inferred using the "CellChat" package [33]. CellChat encompasses a comprehensive molecular signaling database, basing on known structural composition of receptor-ligand interactions. We compared the number of inferred interactions and interaction strength between two phenotype-related cells and visualized significantly altered signaling pathways.

2.17. Natriuretic peptide system in ECTs

ECTs, composed of cardiomyocyte and fibroblasts, provide more physiological platforms for cardiovascular disease modeling. RNA-seq data of ECTs with wild type, heterozygous and homozygous MYBPC3 mutations were acquired from GSE224129 [34]. We visualized the expression levels of members in natriuretic peptide system as heatmap.

2.18. Time series clustering analysis

To estimate transcriptomic alteration during the transformation from fibroblast to myofibroblast, time series RNA-seq data from TGF-β1-treated cardiac fibroblasts were analyzed [35]. "ClusterGVis" package was used for clustering time series gene expression data and genes of natriuretic peptide system were annotated.

2.19. Mendelian randomization

Genome wide association study (GWAS) summary data of CORIN and heart failure and hypertrophic cardiomyopathy was obtained from the IEU Open GWAS project (https://gwas.mrcieu.ac.uk/). Two datasets based on European population (finn-b-I9_HEART-FAIL_AND_HYPERTCARDIOM, eqtl-a-ENSG00000145244) were taken for mendelian randomization (MR) analysis. The finn-b-I9_HEARTFAIL_AND_HYPERTCARDIOM dataset included 304 HF and HCM cases and 218,236 controls, with a depth of 16,380,449 single nucleotide polymorphisms (SNPs). CORIN-related SNPs were acquired from the eqtl-a-ENSG00000145244 dataset, which detected 17,485 SNPs from 31,684 participants. Furthermore, we screened the SNPs associated with CORIN at the genome-wide significance level ($p < 1 \times 10–3$), clumping window >5000 kb, and the linkage disequilibrium level ($r2 < 0.01$). We applied inverse variance weighted (IVW) method as the primary method to evaluate the causal effect and verified the consequence of IVW with MR-Egger, weighted median, weighted model and simple model. Leave-one-out analysis, heterogeneity analysis and pleiotropy

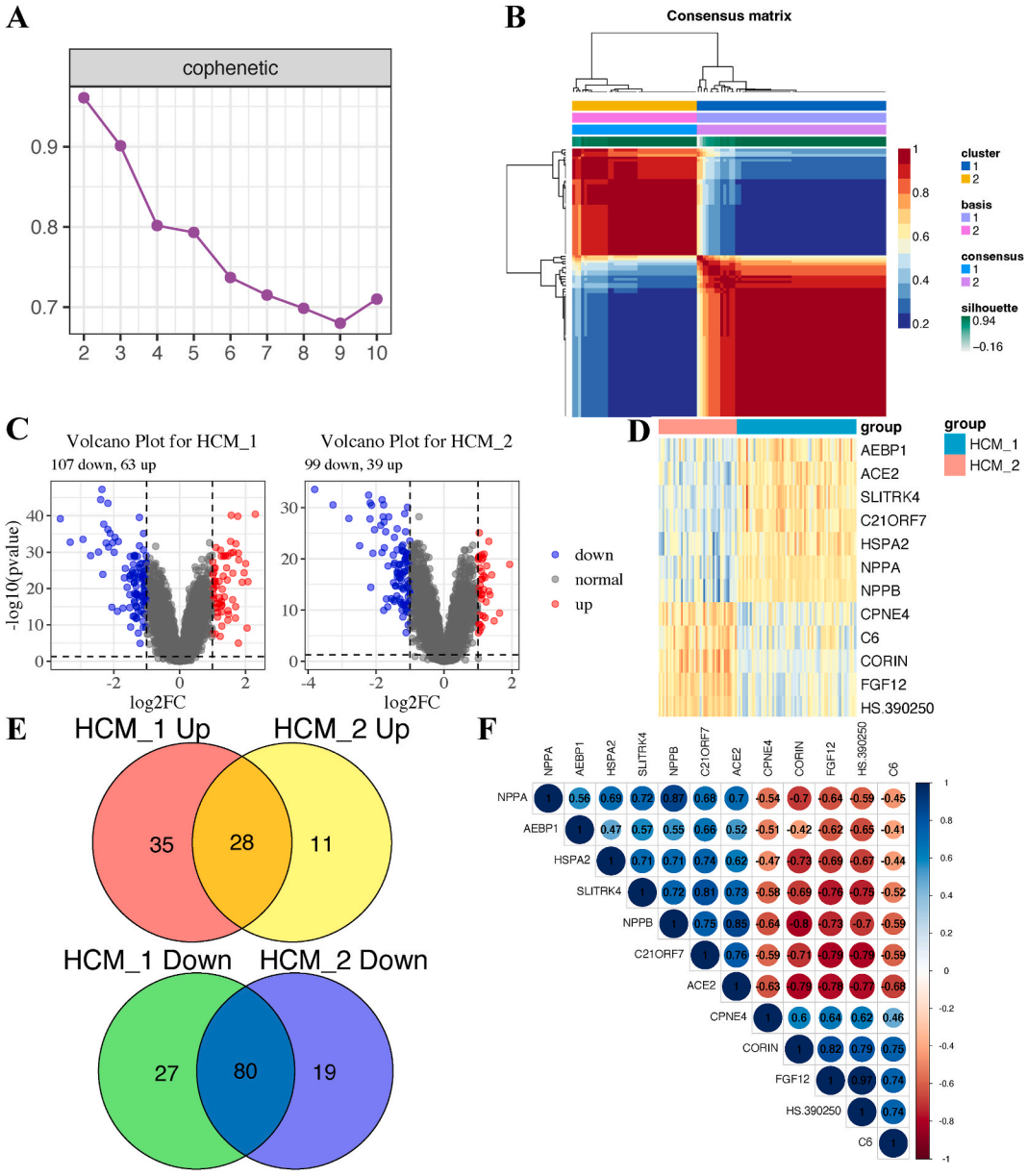

Fig. 1. Identification of HCM subtypes using non-negative matrix factorization. (A) The cophenetic correlation coefficients for the k parameter from 2 to 10. (B) Consensus map of NMF clustering. (C)Volcano plots of DEGs in HCM subtypes compared with control group. (D) Heatmap shows the main DEGs between HCM subtypes. (E) Venn plots of shared DEGs in HCM subtypes. (F) Correlation coefficients among main DEGs between HCM subtypes.

analysis were performed to measure the sensitivity of results. MR procedures were performed with the "TwoSampleMR" package.

2.20. Reagents and antibodies

Recombinant human TGF-β1 and primary antibodies against corin, col1a1, α-SMA were purchased from Abclonal (Wuhan, China). The plasmid, encoding human CORIN NM_006587, was purchased from YouBio (Hunan, China).

Isolation and treatment of neonatal rat cardiac fibroblasts (NRCFs)

Primary NRCFs were isolated from 1- to 3-day-old Sprague-Dawley rats as previously described [36]. Then, cells were cultured in Dulbecco's modified Eagle's medium (DMEM) with 10 % fetal bovine serum (FBS) and penicillin (100 IU/mL)/streptomycin (100 μg/mL). NRCFs were transfected with the CORIN expression vector and replaced with serum-free medium for 6h. From 24h after transfection, NRCFs were exposed to 10 ng/ml TGF-β1 for 48h.

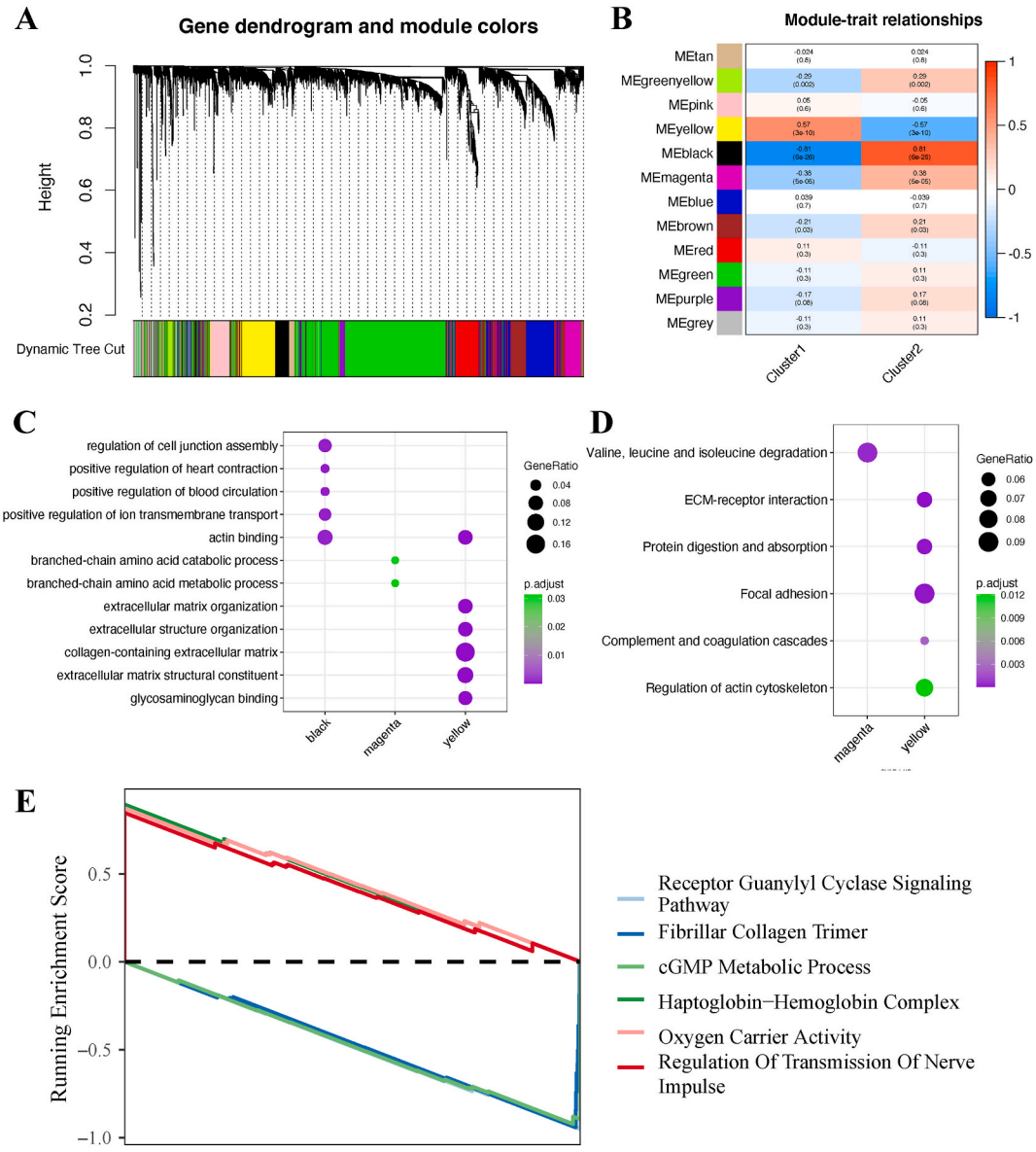

Fig. 2. Weighted gene co-expression network analysis. (A) Clustering dendrogram of genes. (B) Heatmap of module-trait associations. Genes in HCM subgroup related modules were enriched to GO (C) and KEGG pathways (D). (E) GSEA based on expression difference between HCM clusters.

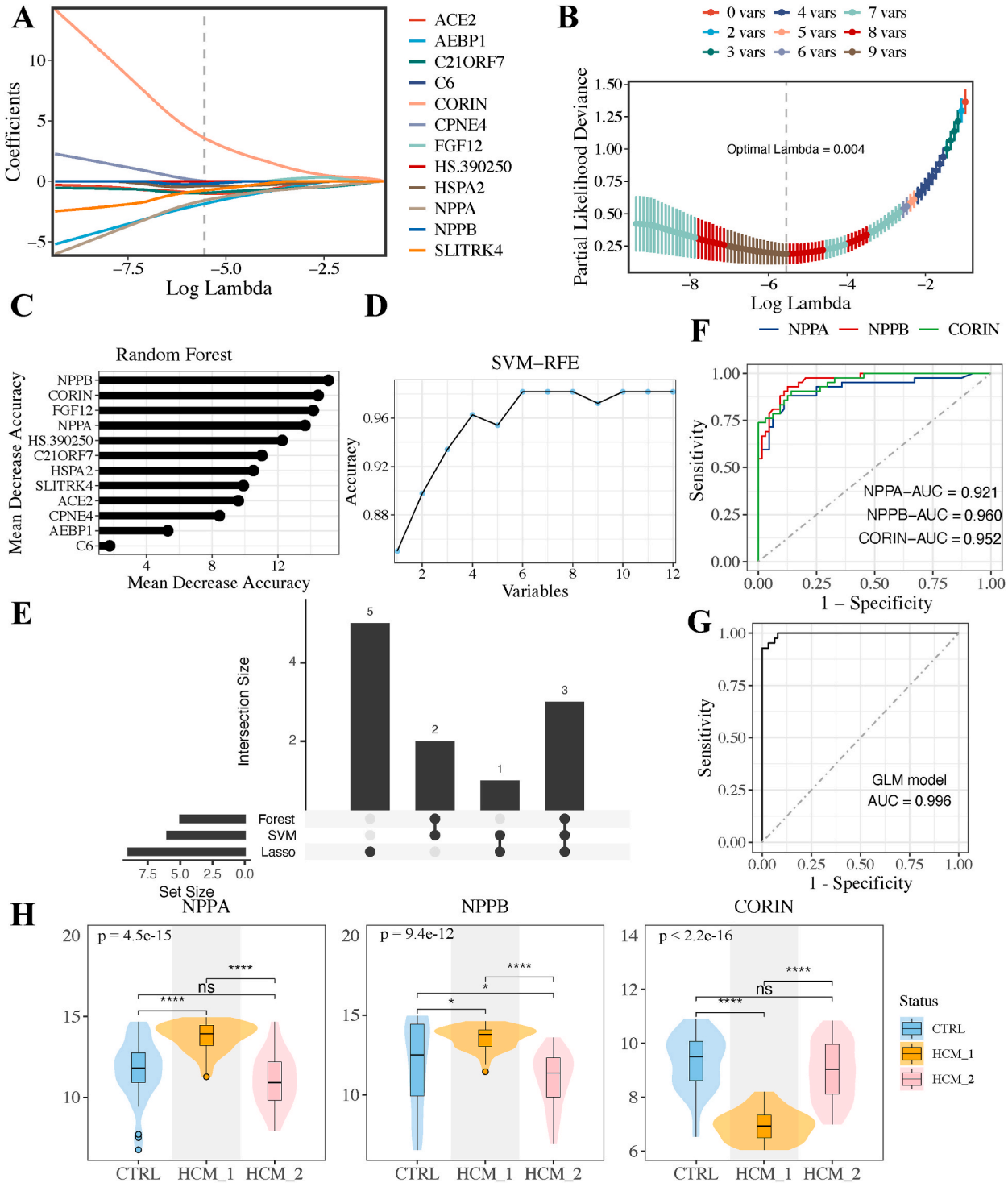

Fig. 3. Hub gene selection with machine learning methods. (A) LASSO coefficient values of the HCM subgroup DEGs. (B) Cross validation of lambda selection and the corresponding variables. (C) Lollipop figure showing feature importance from random forest model. (D) SVM-RFE model accuracy with different variables. (E) UpSet plot presenting the intersection of results from three methods. (F) ROC assays for NPPA, NPPB and CORIN in HCM clusters. (G) ROC assay for the multi-factor model in HCM clusters. (H) Expression levels of NPPA, NPPB and CORIN in control and HCM samples.

2.21. Western Blotting

Western blot analyses were conducted to examine protein changes in NRCFs from various treatment groups. Protein extraction and western blots were performed according to procedures detailed in our previous studies [37]. The gray value data of the immunoblots was quantified using ImageJ software (NIH Image, USA).

2.22. Statistical analysis

Bioinformatic analyses were performed using R version 4.2.2. Statistical methods used in these analyses have been detailed above. For the Western blot data, values are expressed in the form of means ± standard error. Student's t-test or one-way ANOVA was used to identify significant differences between groups where appropriate. GraphPad Prism 8 (GraphPad Software, Inc., San Diego, CA, USA) was employed for calculations and visualizations.

3. Results

3.1. Identification of HCM clusters with NMF

According to the "Muscle contraction-Cardiac conduction" pathway, we applied NMF on 106 myocardial samples from the HCM cohort GSE36961. The cophenetic correlation coefficients for factorization rank from 2 to 10 were presented in Fig. 1A. The cophenetic coefficient began to decrease when the rank = 2. Consequently, 106 HCM patients were divided into 2 distinct clusters (Fig. 1B). Cluster 1 (n = 64) and Cluster 2 (n = 42) shared similar age composition (45.50 vs. 52.00, p = 0.51), while there were fewer women in Cluster 2 (42.2 % vs. 64.3 %, p = 0.04). For their transcriptional differences, Cluster 1 presented higher levels of NPPA and NPPB transcripts, which is a hallmark of heart failure.

In comparing HCM Cluster 1 and Cluster 2 with the control group, we identified 170 DEGs (63 up-regulated, 107 down-regulated) and 138 DEGs (39 up-regulated, 99 down-regulated) respectively (Fig. 1C–Supplementary Table S2, Supplementary Table S3). Additionally, the comparison between HCM subgroups identified 12 DEGs (7 up-regulated in Cluster 1, 5 up-regulated in Cluster 2), which were visualized as heatmap (Fig. 1D–Supplementary Table S4). We further observed that 28 up-regulated and 80 down-regulated DEGs were common in HCM Clusters (Fig. 1E), which were mainly involved in immune and inflammation. DEGs between clusters displayed high relativity (Fig. 1F), suggesting a joint signaling pathway.

3.2. Co-expression module construction and enrichment analysis in HCM clusters

WGCNA was applied to cluster genes into gene modules with similar expression pattern, which allowed linking gene modules with clinical traits. After clustering and merging similar modules, we identified 12 modules (Fig. 2A).

We then visualized the module-trait relationships with Spearman correlation coefficients. Three modules were found significantly associated with HCM clusters. Specifically, the "yellow" module (corr = 0.57, p = 3e-10) was positively correlated with Cluster 1, while the "black" (corr = 0.81, p = 6e-26) and "magenta" (corr = 0.38, p = 5e−5) modules were positively correlated with Cluster 2 (Fig. 2B).

As depicted in Fig. 2C, genes in the "black" module were primarily involved in cell junction assembly, actin binding, positive regulation of heart contraction, blood circulation and ion transmembrane transport. The "magenta" module was related to the metabolism and catabolism of branched-chain amino acid. The "yellow" module, on the other hand, was related to the regulation and function of extracellular matrix (ECM). Moreover, the results of KEGG enrichment analysis validated these (Fig. 2D).

Lastly, GSEA performed between HCM clusters revealed that HCM Cluster 1 features receptor guanylyl cyclase signaling pathway, cGMP metabolic process and fibrillar collagen trimer. While HCM Cluster 2 features haptoglobin-hemoglobin complex, oxygen carrier activity and regulation of transmission of nerve impulse (Fig. 2E).

3.3. Identification of characteristic genes of HCM clusters

Three ML methods were employed to screen out hub genes that differentiate HCM clusters. For LASSO regression, the coefficients of variables were calculated at different lambda values (Fig. 3A). Through tenfold cross-validation, we selected the largest value of lambda that keeps error within one standard error of the minimum ($\lambda = 0.04$), which resulted in the selection of 9 variables (SLITRK4, CORIN, C21ORF7, ACE2, NPPA, HSPA2, AEBP1, NPPB, CPNE4) (Fig. 3B). Through random forest algorithm, five genes (NPPB, CORIN, FGF12, NPPA, HS.390250) with mean decrease accuracy larger than 12 were picked (Fig. 3C). Meanwhile, 6 variables (FGF12, NPPB, NPPA, CORIN, HS.390250, C21ORF7), identified by fivefold CV, ahcieved the highest accuracy in SVM-REF model (Fig. 3D). By integrating the results from random forest, SVM-RFE and LASSO regression, we selected NPPA, NPPB and CORIN as characteristic genes (Fig. 3E).

ROC curves were constructed to assess the diagnostic values of these characteristic genes and a comprehensive model. All three hub genes could effectively differentiate HCM clusters (NPPA: 0.921; NPPB: 0.960; CORIN: 0.952) (Fig. 3F). Moreover, the generalized linear model incorporating these three genes had even higher accuracy (AUC = 0.996) (Fig. 3G). After detecting the transcript levels of NPPA, NPPB and CORIN, we found that HCM Cluster 1 showed higher NPPA, NPPB levels but lower CORIN level (Fig. 3H). Interestingly, HCM Cluster 2 exhibited a closer expression pattern to the control group, showing no significant difference as in NPPA and

CORIN expression.

3.4. Identification of clinical phenotype and relative factors

Trajectory inference method was employed to recognize the clinical features of HCM clusters. Transcription profiles of HCM clusters and control were used for dimension reduction and then trajectory fitting based on DEGs in HFrEF (Fig. 4A). However, HFpEF-related DEGs can't distinguish control and HCM clusters well (data not shown). The inferred trajectory revealed continues increases of NPPA, NPPB and decrease of ACE2, CORIN from Cluster 2 to Cluster 1 (Fig. 4B).

On comparing gene expression levels, we found that CORIN increased in HFpEF and decreased in severe HFrEF but not in HFrEF cases with LVEF ≥20. Another natriuretic peptide convertase, FURIN, decreased in both HFpEF and HFrEF. Natriuretic peptide NPPA increased in both HFpEF and HFrEF, while NPPB only increased in HFrEF (Fig. 4C). Considering the distinct trend, we fitted the

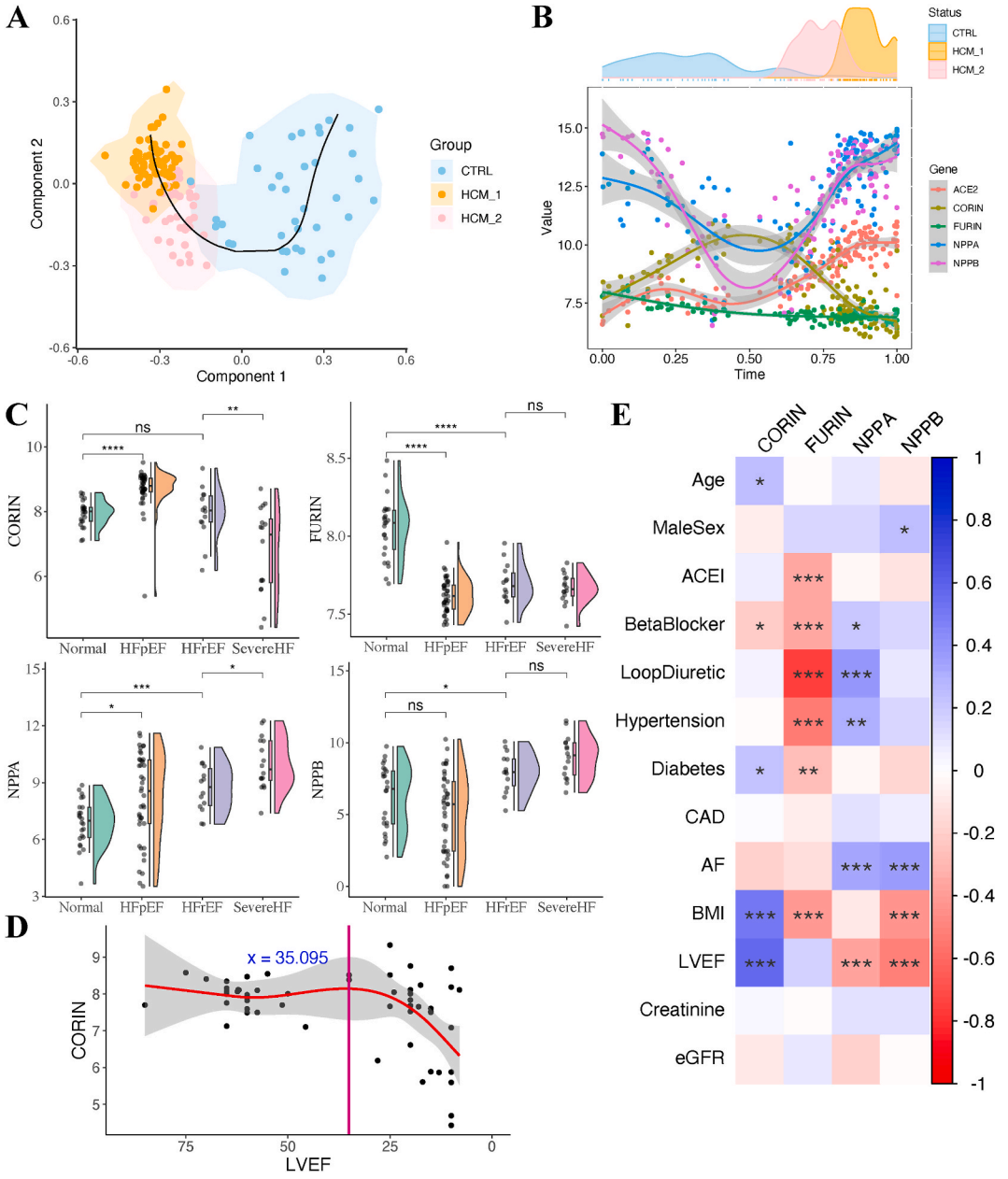

Fig. 4. Inference of HCM trajectory to HFrEF. (A) HFrEF-like disease trajectory was inferred after dimensionality reduction. (B) Gene expression trends according to inferred trajectory. (C) Gene expression levels of characteristic genes. (D) Association between LVEF and CORIN levels using RCS model. (E) Correlation coefficients between hub genes and clinical characteristics.

association between LVEF and CORIN expression with RCS method. It recommended that CORIN expression started to decline when LVEF = 35 (Fig. 4D). Additionally, the correlation coefficients between genes and clinical features were shown in Fig. 4E.

3.5. Alteration of cell types between HCM clusters

The fractions of cell types in myocardial tissues from HCM patients were estimated and compared between clusters. Accordingly, the fractions of dendritic cell and endothelial cell were higher in HCM Cluster 2, while fibroblasts and neuronal cells were more abundant in HCM Cluster 1 (Fig. 5A). We also presented the correlations between cell types and DEGs in Fig. 5B. Then, the fractions of cell types were mapped into the inferred trajectory, suggesting an increase of fibroblasts in HCM Cluster 1 (Fig. 5C). Consistently, differential abundance analysis on HCM snRNA-seq data suggested that epicardial cell, cardiomyocyte and adipocyte were more abundant in HCM Cluster 2 and activated fibroblast was enriched in Cluster 1 (Fig. 5D and E).

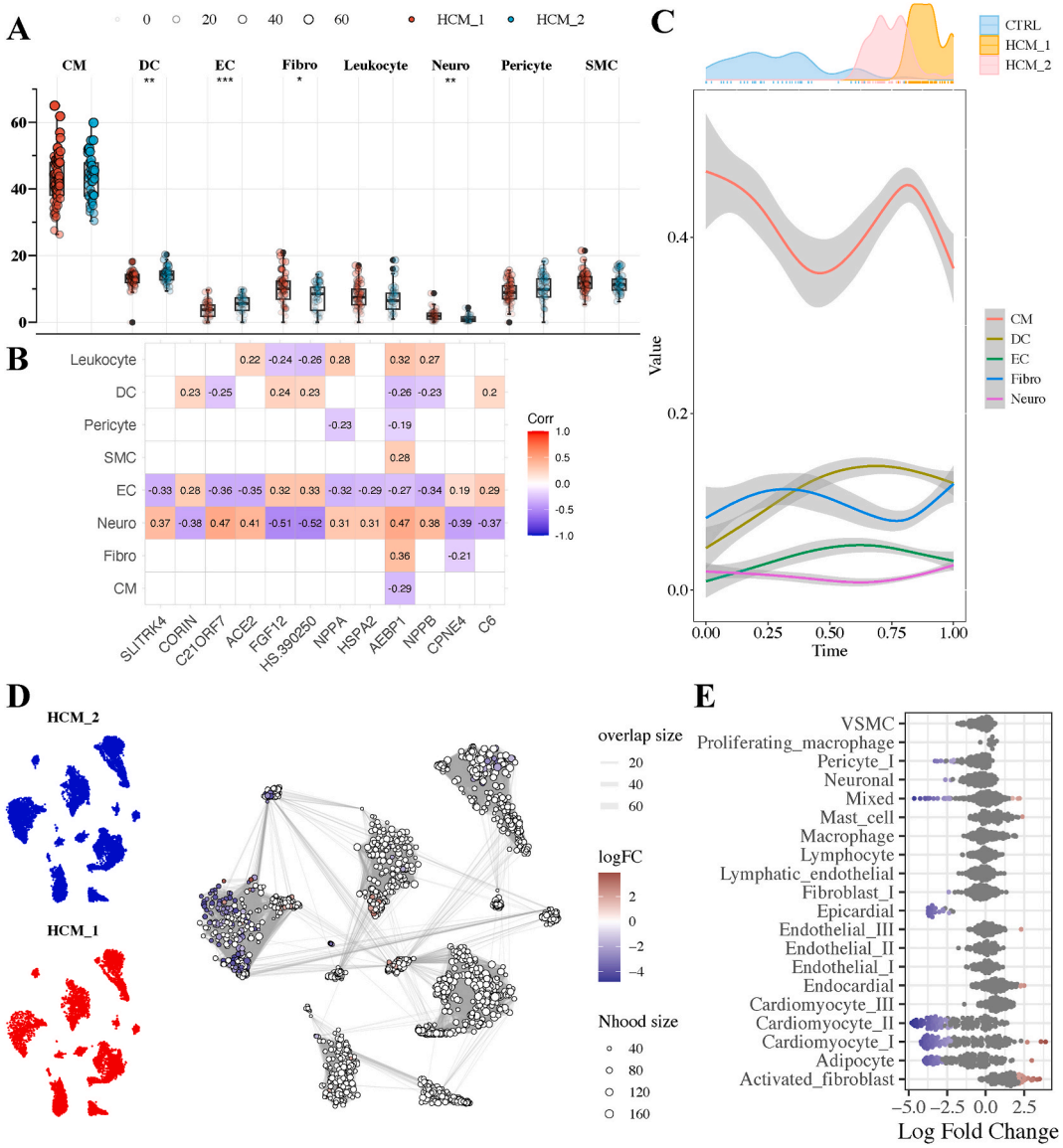

Fig. 5. Cell composition differs between HCM clusters. (A) Comparisons of inferred cell type fraction between HCM Clusters. (B) Associations between cell types and genes. (C) Cell composition trends according to inferred trajectory. (D) Differential abundance analysis of HCM clusters. (E) Beeswarm plot shows differential abundance of cell types.

3.6. Communication differences in cells associated with HCM clusters

We used the SCISSOR algorithm to verify the association between cell types and HCM clusters. This algorithm identified that HCM Cluster 1 associated cells were mainly fibroblasts, activated fibroblasts, cardiomyocytes III, neuronal cells and vascular smooth muscle

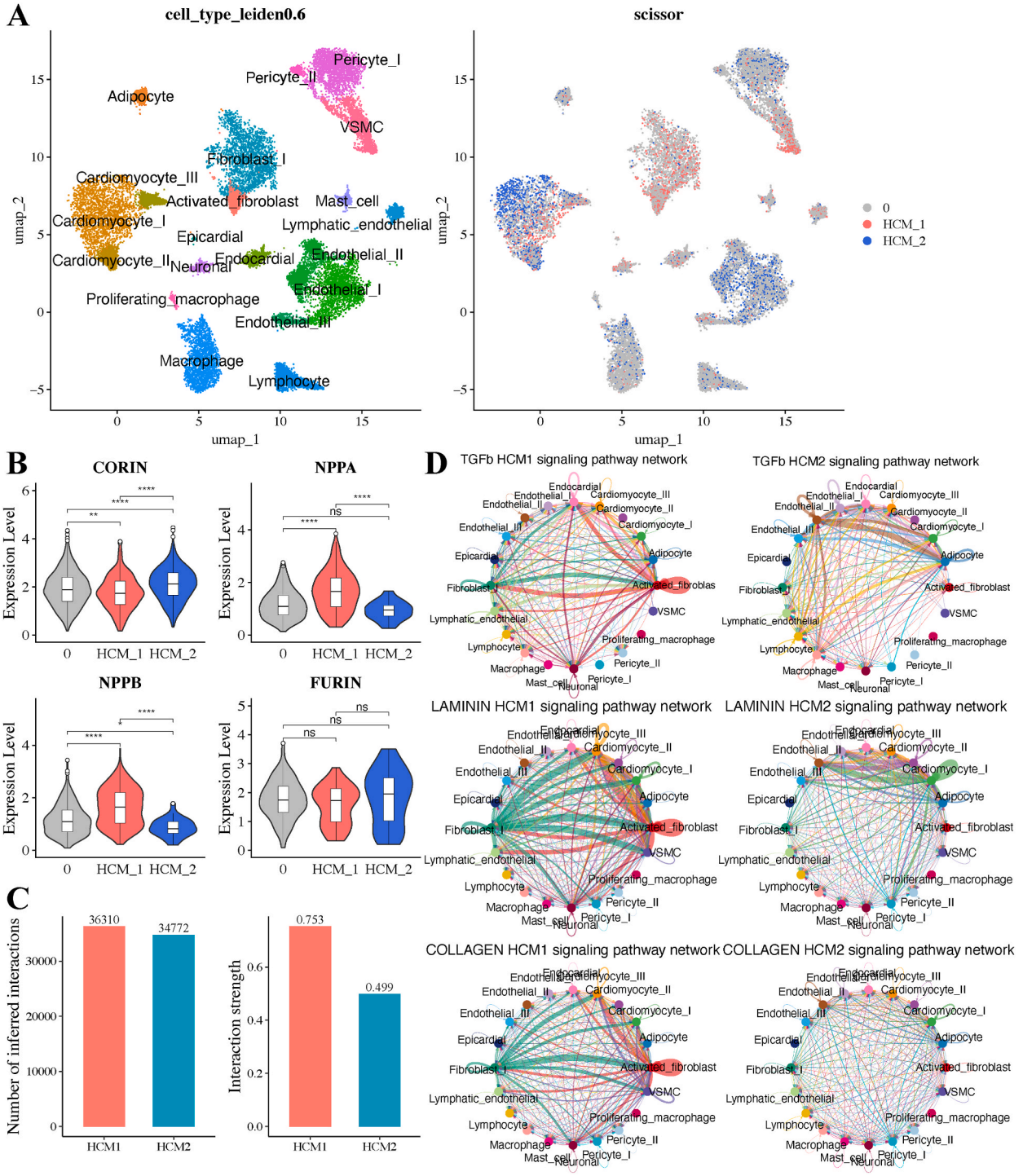

Fig. 6. Results of Scissor algorithm and CellChat at single cell resolution. (A) Identification of HCM cluster related cell types. (B) Expression levels of genes in HCM cluster-related cells. (C) Total interaction strength between HCM clusters. (D) Circle plots exhibiting the differences in the interaction strength of TGFb (above), Laminin (middle) and Collagen (below) signaling pathways between HCM Clusters.

cells (Fig. 6A). Conversely, cardiomyocytes I, II and endothelial I, II were associated with HCM Cluster 2. Compared with background and Cluster 2 related cells, NPPA and NPPB were elevated in Cluster 1 related cells, and CORIN was down-regulated (Fig. 6B).

Subsequently, cell-cell communication networks were individually constructed in Cluster 1 and 2 related cells. Both the number of inferred interactions and interaction strength were elevated in HCM Cluster 1 (Fig. 6C). Specifically, TGFβ, LAMININ and COLLAGEN signaling pathways, mainly mediated by fibroblasts and activated fibroblasts, were enriched in HCM Cluster 1, indicating a profibrotic status (Fig. 6D).

3.7. Phenotype verification in DCM

Given the heterogeneity and similarity within the spectrum of cardiomyopathies, we conducted equivalent analyses on DCM. In the DCM cohort GSE141910, the NMF algorithm divided patients into two clusters, with CORIN being down-regulated in DCM, especially in DCM Cluster 1 (Supplementary Figs. S1A and B). Similarly, patients in the DCM cohort GSE135055 were classified into Cluster 1 (n

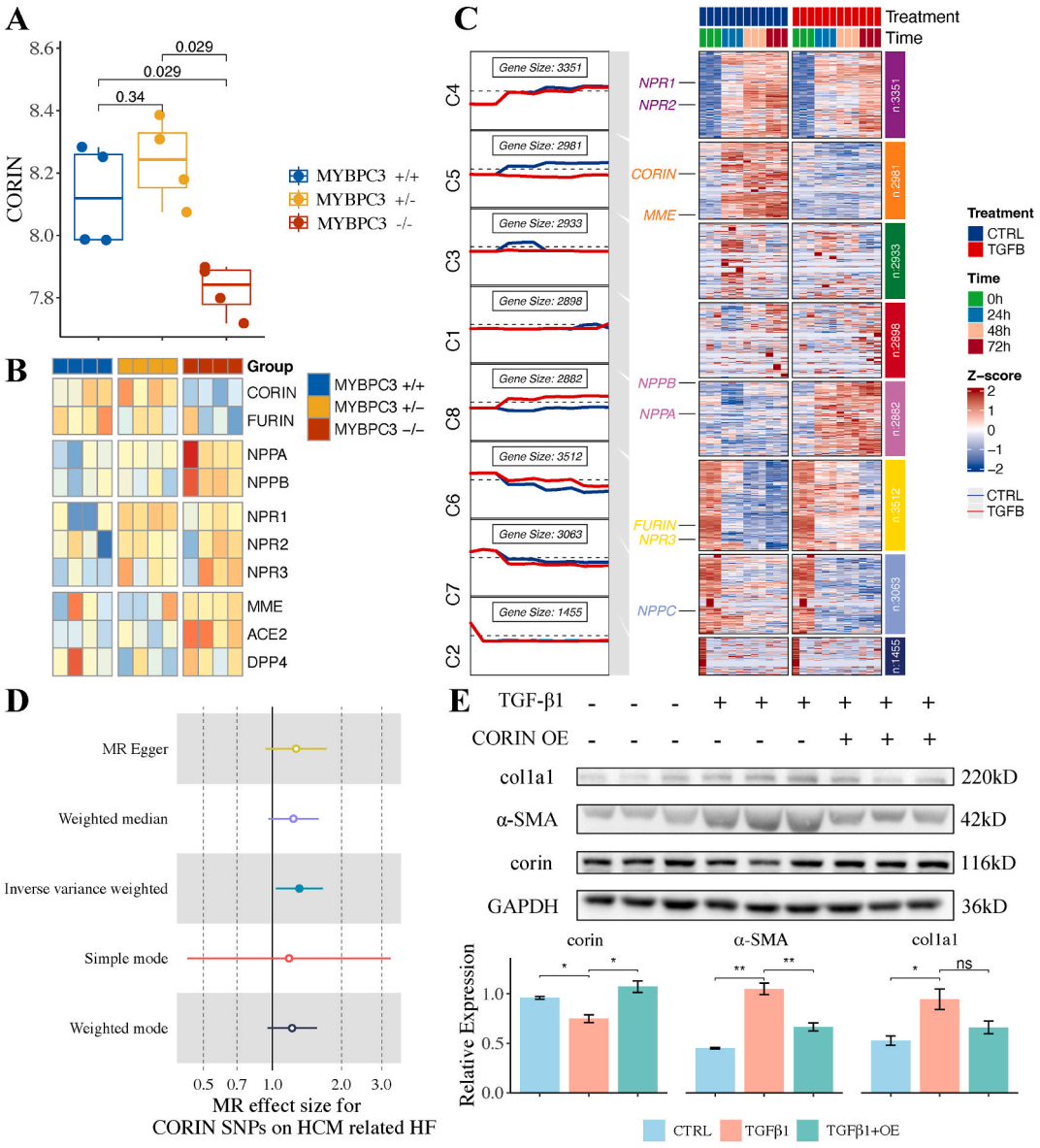

Fig. 7. CORIN deficiency in the activation of cardiac fibroblasts. (A) CORIN expression in MYBPC3-mutated ECTs. (B) Fibrosis markers in MYBPC3-mutated ECTs. (C) Time series clustering of transcriptomic profile in cardiac fibroblasts. (D) Mendelian randomization analysis of CORIN mutations' effect on HCM related HF. (E) Western blot assay confirmed that, compared with control group, the protein levels of representative fibroblast activation markers in NRCF were increased by TGF-β1 treatment and mitigated by CORIN overexpression. *P < 0.05, **P < 0.01, one-way ANOVA test.

= 10) and Cluster 2 (n = 8) (Supplementary Fig. S1C). Due to sample size limitations, comparisons of baseline characteristics only suggested a lower LVEF in Cluster 1 (median of 23.50 vs. 31.00, p = 0.043) (Supplementary Table S5). Based on our molecular subtype classification, survival analysis identified that patients in DCM Cluster 1 might be confronted with significantly shorter duration from symptom initiation to heart transplantation (p = 0.01) (Supplementary Fig. S1D).

HFrEF trajectory was inferred on the clustered GSE141910 cohort and fitted well (Supplementary Fig. S2A). Gradual Increases in NPPA, NPPB and a decrease in CORIN were confirmed in the inferred trajectory (Supplementary Fig. S2B). From differential abundance analysis, we confirmed that DCM Cluster 1 also features abundant activated fibroblasts (Supplementary Figs. S3A and B). Slightly different from HCM, cardiomyocyte I and III were also more abundant in DCM Cluster 1 as well. In addition, the Scissor algorithm identified that DCM Cluster 1 was associated with fibroblasts and adipocytes while Cluster 2 was associated with cardiomyocytes (Supplementary Fig. S3C).

3.8. CORIN deficiency is involved in cardiac fibrosis and heart failure

Based on the above results, we identified cardiac fibroblasts as potential mediators in HCM Cluster 1 and corin as an anti-fibrotic target. We utilized the MYBPC3 mutated human ECTs dataset GSE224129 and found that CORIN was significantly decreased in mutant homozygotes (Fig. 7A). The expression levels of other members of the natriuretic peptide system were visualized in Fig. 7B, presenting a pathological state with low levels of natriuretic peptide-converting enzymes, high levels of natriuretic peptides and their catabolic enzymes. In the time series TGFβ1-treated culturing human cardiac fibroblasts RNA-seq dataset GSE225336, genes were clustered into 8 clusters and compared between control and TGF-β1 stimulated groups. CORIN expression in human cardiac fibroblasts increases during in vitro culture, while this alteration can be almost completely blocked by TGF-β1 (Fig. 7C). The IVW model using 36 CORIN-related SNPs conformed that genetic variants of CORIN were significantly associated with an increased risk of HCM related HF (OR: 1.311; 95 % CI: 1.002–1.619; p = 0.024) (Fig. 7 D). Meanwhile, MR analyses with other models (MR Egger, Weighted median, simple mode, Weighted mode) showed similar but non-significant results. Leave-one-out and pleiotropy tests were presented in Table S6. In NRCFs, the protein level of corin was down-regulated by TGF-β1. And overexpression of CORIN could mitigate TGF-β1-mediated increase of profibrotic markers (Fig. 7E).

4. Discussion

In this study, we employed the NMF algorithm to categorize bulk RNA-seq data from HCM and DCM patients. Our results subdivided HCM patients into 2 clusters with distinct transcriptional characteristics, similar results were found in DCM populations as well. Intriguingly, one cluster exhibited a transcriptional profile similar to HFrEF, characterized by reduced CORIN expression, proliferation and activation of fibroblasts. Additionally, overexpression of CORIN was found to mitigate TGF-β1-mediated increase of fibroblast activation markers in NRCF. These findings may provide new insights into the molecular heterogeneity among HCM (and DCM) patients, and further evidenced the therapeutic potential of corin for cardiomyopathies and HFrEF.

Cardiomyopathies represent a diverse group of heart muscle diseases, which exhibit clinical symptoms of HF at advanced stage [38]. Contemporary management strategies have significantly improved the clinical course of HCM, resulting in a low disease-related mortality rate of 0.5 %/year [39]. Current evidences suggested that certain cardiomyopathy patients were more likely to develop HF. For instance, HCM patients with homozygous MYBPC3 mutation at the genetic level or left ventricular outflow tract obstruction at the phenotype level were more susceptive to HF development [40,41]. Hence, subdivision of cardiomyopathies has long been concerned and has been respectively performed on HCM and DCM. Liang et al. proposed four HCM molecular subtypes based on venous blood proteomics profiling through unsupervised ML methods [42]. Recently, DCM subtypes were recommended based on clinical, proteomic, genetic and transcriptomic features [43,44]. Contractile dysfunction occurs in the advanced stages of both HCM and DCM, indicating the deterioration of cardiomyopathy. Here, we selected the “Muscle contraction-Cardiac conduction” pathway to cluster HCM patients. Besides, pathways such as lipid metabolism, ferroptosis, oxidative stress were tested for cluster, while samples couldn’t be explicitly divided. Interestingly, results from the above studies all identified a profibrotic subtype in HCM or DCM, resembling the Cluster 1 in our work. HCM Cluster 1 was enriched with ECM remodeling and organization, consistent with enrichment results of other profibrotic subtypes. Considering clinical phenotypes, clustering of DCM cohort GSE135055 identified lower LVEF and worse prognosis for Cluster 1 patients. Thus, the identification of a Cluster 1 characterized with profibrotic status and negative inotropic effect is a key finding of this study.

Regarding Cluster 2, enrichment analysis identified its features in the branched-chain amino acid metabolic process and valine, leucine and isoleucine degradation. In contrast, Vakrou et al. compared the molecular phenotype of HCM mouse model with that of HCM patients (the same data source as our work), only revealing similar enrichment in valine, leucine and isoleucine degradation [45]. However, the R92W-TnT mouse model can well embody HCM Cluster 2 considering enriched pathways. This suggests that HCM is a variable condition and current animal models merely simulate it from different perspectives.

Based on NMF clustering and differential expression analysis, totally 12 DEGs were identified. Besides the selected hub genes, other DEGs may represent multiple aspects of differences between clusters. Thereinto, ACE2 was also involved in the metabolism of natriuretic peptides [46]. From the same data source, Bos et al. found marked up-regulation of ACE2 in cardiac tissues from HCM patients and proposed an increased risk for COVID-19 manifestations and outcomes [47]. Here, we identified stepwise up-regulated transcript abundance of ACE2, recommending advanced HCM status and higher susceptibility towards SARS-CoV-2 for patients in HCM Cluster 1. However, further inferences need to be combined with clinical information and larger cohort studies. Meanwhile, another study revealed a linear-specific regulatory role of AEBP1 in HCM based on snRNA-seq. Down-regulation of AEBP1 promoted

the activation of cardiac fibroblasts in vitro [48]. These transcriptomic variations may collectively contribute to differences between subtypes of cardiomyopathies.

4.1. The progression of cardiomyopathy to HF

According to our results, the recognized HCM and DCM Cluster 1 were characterized with higher NPPA and NPPB, classic characteristics of HF. Although corresponding clinical information of patients in GSE36961 was ambiguous, we retrieved the general demographics of the same cohort analyzed [47]. For the 106 HCM patients, the median ejection fraction was 74 % (interquartile range, 68–77 %), and 77 % (n = 82) had NYHA class III to IV symptoms. Consistently, the application of trajectory inference indicated that healthy control and cardiomyopathy cases can be well fitted in the HFrEF progression. Recently, several hypotheses about the molecular biological mechanisms underlying development from cardiomyopathy to HFrEF have been raised, such as myofibroblast transformation, mitochondrial injury and microvascular dysfunction [49–51]. Inspired by the results of cell composition analysis, we found differential abundance and activation of fibroblasts between clusters and focused on cardiac fibrosis in further analyses.

Cardiac fibroblast is an essential cell type in the heart and involved in the genesis and development of HF [52]. Mutation of MYBPC3, a common pathogenesis in HCM, has been proved to mediate the activation of cardiac fibroblasts through the TGF-β pathway [53,54]. However, the role of natriuretic peptides in fibroblast transformation remains unclear.

The natriuretic peptide system involves natriuretic peptides, their receptors and processing enzymes and has become of increasing interest as a biotarget for HF [55]. NPPA and NPPB respectively encode A-type natriuretic peptide and BNP, which are secreted by the heart in their precursor molecules (pro-ANP, pro-BNP) [56]. CORIN encodes corin, a transmembrane cardiac serine protease. Corin acts as a natriuretic peptide-converting enzyme, mediating cleavage of pro-ANP and pro-BNP [57]. Plasma corin levels was formerly identified correlated with the severity of HF [58]. In addition, in HFrEF patients from DCM, depressed corin levels indicated an early systolic dysfunction before increases of ANP/BNP, and were correlated with increased circulating uncleaved pro-ANP levels [59,60]. Similarly, deficiency of corin influences the activation of ANP and BNP, perturbing body fluid homeostasis and myocardial preservation [61]. FURIN encodes furin, paired basic amino acid cleaving enzyme, another convertase of natriuretic peptides [62]. We found the expression of FURIN was down-regulated in both clusters, indicating a lack of natriuretic peptide activation in cardiomyopathy. Considering the decreased CORIN and the amplification of NPPA and NPPB transcripts, this deficiency might be more serve in Cluster 1. We further selected cardiac fibroblasts as a target and verified that overexpression of corin can reverse fibroblast activation. Accordantly, former studies have established that overexpression or addition of recombinant corin can ameliorate heart failure symptoms and cardiac fibrosis in DCM and HF mouse models [63,64]. Thus, research into corin-related treatment is promising and urgently needed. This study identified transcriptional subclusters of HCM and DCM, and suggested an anti-fibrotic role of corin in cardiac fibroblasts.

4.2. Limitations

While our study provides novel insights into the molecular subtypes of HCM and DCM, and the potential role of CORIN in the development of HFrEF, several limitations should be acknowledged. Firstly, our study relied solely on publicly available microarray and RNA-seq data of HCM and DCM patients, and did not include data from our own patient cohort. The lack of imaging data limited the estimation of LVEF among patients from main HCM and DCM cohorts. Secondly, the clustering of cardiomyopathy was not validated using experimental methods. Thirdly, we did not delve into the downstream pathway of CORIN in cardiac fibroblasts, which could have provided a more comprehensive understanding of the underlying molecular mechanisms. Finally, the lack of corresponding clinical information for the involved cases limited our ability to establish associations between transcriptome features and clinical phenotypes.

5. Conclusion

In conclusion, our study, utilizing the NMF algorithm, has identified two distinct molecular subtypes in HCM and DCM, providing a new perspective on the heterogeneity of cardiomyopathies. Importantly, we recognized a profibrotic and HFrEF-like Cluster 1 and substantiated its characteristics at molecular and cellular levels. Consistently, we further evidenced that CORIN deficiency was presented in cardiomyopathies and HFrEF. Furthermore, our findings suggest the therapeutic potential of manipulating CORIN expression in cardiac fibroblasts. These results proposed molecular subtypes of HCM and DCM, and indicated the anti-fibrotic role of corin in cardiac fibroblasts. Future research should aim to validate these findings in larger, independent cohorts and explore the therapeutic implications of CORIN in more depth.

Ethics approval and consent to participate

The databases are publicly available and open access, and the present study followed the data access policy and publishing guidelines of these databases. Therefore, no local ethics committee is required to approve this study.

Consent for publication

Not applicable.

Data availability statement

The datasets generated and/or analyzed during the current study are available and detailed in Supplementary Table S1. Data associated with my study was not deposited into a publicly available repository. Data will be made available on request.

Funding

This research is funded by the National Natural Science Foundation of China (Grant No. 81700251).

Ethical approval

The patient data analyzed in this work were acquired from publicly available datasets.

CRediT authorship contribution statement

Jun-yan Kan: Data curation. **Dong-chen Wang:** Data curation. **Zi-hao Jiang:** Writing – original draft. **Li-da Wu:** Methodology. **Ke Xu:** Investigation. **Yue Gu:** Conceptualization.

Declaration of competing interest

The authors declare that they have no known competing financial interests or personal relationships that could have appeared to influence the work reported in this paper.

Acknowledgements

The authors thank Dr Qi-tao Chen for helping with the English language improvement.

Abbreviations

HCM Hypertrophic cardiomyopathy
DCM Dilated cardiomyopathy
HF Heart failure
HFrEF Heart failure with reduced ejection fraction
LVEF Left ventricular ejection fraction
NMF Non-negative matrix factorization
RNA-seq RNA sequencing
snRNA-seq Single-nucleus RNA sequencing
ECT Engineered cardiac tissue
GEO Gene Expression Omnibus
DEG Differentially expressed gene
log2FC Log2 fold change
FDR False discovery rate
GSEA Gene set enrichment analysis
GO Gene ontology
KEGG Kyoto encyclopedia of genes and genomes
WGCNA Weighted gene co-expression network analysis
SVM-RFE support vector machines-recursive feature elimination
LASSO Least absolute shrinkage and selection operator
ROC: Receiver operating characteristic
AUC Area under ROC curve
HFpEF Heart failure with preserved ejection fraction
NRCF Neonatal rat cardiac fibroblast
DMEM Dulbecco's modified Eagle's medium
FBS Fetal bovine serum

Appendix A. Supplementary data

Supplementary data to this article can be found online at https://doi.org/10.1016/j.heliyon.2024.e37838.

References

[1] S.R. Ommen, C. Semsarian, Hypertrophic cardiomyopathy: a practical approach to guideline directed management, Lancet 398 (2021) 2102–2108, https://doi.org/10.1016/S0140-6736(21)01205-8.

[2] D. Reichart, C. Magnussen, T. Zeller, S. Blankenberg, Dilated cardiomyopathy: from epidemiologic to genetic phenotypes: a translational review of current literature, J. Intern. Med. 286 (2019) 362–372, https://doi.org/10.1111/joim.12944.

[3] M.J. Daniels, L. Fusi, C. Semsarian, S.S. Naidu, Myosin modulation in hypertrophic cardiomyopathy and systolic heart failure: getting inside the engine, Circulation 144 (2021) 759–762, https://doi.org/10.1161/CIRCULATIONAHA.121.056324.

[4] B.J. Maron, J.M. Gardin, J.M. Flack, S.S. Gidding, T.T. Kurosaki, D.E. Bild, Prevalence of hypertrophic cardiomyopathy in a general population of young adults: echocardiographic analysis of 4111 subjects in the CARDIA study, Circulation 92 (1995) 785–789, https://doi.org/10.1161/01.CIR.92.4.785.

[5] W.J. McKenna, B.J. Maron, G. Thiene, Classification, epidemiology, and global burden of cardiomyopathies, Circ. Res. 121 (2017) 722–730, https://doi.org/10.1161/CIRCRESAHA.117.309711.

[6] S.P. Murphy, N.E. Ibrahim, J.L. Januzzi, Heart failure with reduced ejection fraction: a review, JAMA, J. Am. Med. Assoc. 324 (2020) 488–504, https://doi.org/10.1001/jama.2020.10262.

[7] H. Tsutsui, Recent advances in the pharmacological therapy of chronic heart failure: evidence and guidelines, Pharmacol. Ther. 238 (2022) 108185, https://doi.org/10.1016/j.pharmthera.2022.108185.

[8] J.M. Bos, V.B. Hebl, A.L. Oberg, Z. Sun, D.S. Herman, P. Teekakirikul, J.G. Seidman, C.E. Seidman, C.G. dos Remedios, J.J. Maleszewski, H. V Schaff, J. A. Dearani, P.A. Noseworthy, P.A. Friedman, S.R. Ommen, F. V Brozovich, M.J. Ackerman, Marked up-regulation of ACE2 in hearts of patients with obstructive hypertrophic cardiomyopathy: implications for SARS-CoV-2–mediated COVID-19, Mayo Clin. Proc. 95 (2020) 1354–1368, https://doi.org/10.1016/j.mayocp.2020.04.028.

[9] X. Hua, Y.Y. Wang, P. Jia, Q. Xiong, Y. Hu, Y. Chang, S. Lai, Y. Xu, Z. Zhao, J. Song, Multi-level transcriptome sequencing identifies COL1A1 as a candidate marker in human heart failure progression, BMC Med. 18 (2020) 1–16, https://doi.org/10.1186/s12916-019-1469-4.

[10] V.S. Hahn, H. Knutsdottir, X. Luo, K. Bedi, K.B. Margulies, S.M. Haldar, M. Stolina, J. Yin, A.Y. Khakoo, J. Vaishnav, J.S. Bader, D.A. Kass, K. Sharma, Myocardial gene expression signatures in human heart failure with preserved ejection fraction, Circulation 143 (2021) 120–134, https://doi.org/10.1161/CIRCULATIONAHA.120.050498.

[11] C.J. Codden, M.T. Chin, Common and distinctive intercellular communication patterns in human obstructive and nonobstructive hypertrophic cardiomyopathy, Int. J. Mol. Sci. 23 (2022), https://doi.org/10.3390/ijms23020946.

[12] M. Chaffin, I. Papangeli, B. Simonson, A.D. Akkad, M.C. Hill, A. Arduini, S.J. Fleming, M. Melanson, S. Hayat, M. Kost-Alimova, O. Atwa, J. Ye, K.C. Bedi, M. Nahrendorf, V.K. Kaushik, C.M. Stegmann, K.B. Margulies, N.R. Tucker, P.T. Ellinor, Single-nucleus profiling of human dilated and hypertrophic cardiomyopathy, Nature 608 (2022) 174–180, https://doi.org/10.1038/s41586-022-04817-8.

[13] W.J. De Lange, E.T. Farrell, J.J. Hernandez, A. Stempien, C.R. Kreitzer, D.R. Jacobs, D.L. Petty, R.L. Moss, W.C. Crone, J.C. Ralphe, cMyBP-C ablation in human engineered cardiac tissue causes progressive Ca2+-handling abnormalities, J. Gen. Physiol. 155 (2023), https://doi.org/10.1085/jgp.202213204.

[14] A.S. Helms, V.T. Tang, T.S. O'Leary, S. Friedline, M. Wauchope, A. Arora, A.H. Wasserman, E.D. Smith, L.M. Lee, X.W. Wen, J.A. Shavit, A.P. Liu, M.J. Previs, S. M. Day, Effects of MYBPC3 loss-of-function mutations preceding hypertrophic cardiomyopathy, JCI Insight 5 (2020), https://doi.org/10.1172/jci.insight.133782.

[15] D. Sean, P.S. Meltzer, GEOquery: a bridge between the gene expression Omnibus (GEO) and BioConductor, Bioinformatics 23 (2007) 1846–1847, https://doi.org/10.1093/bioinformatics/btm254.

[16] M.E. Ritchie, B. Phipson, D. Wu, Y. Hu, C.W. Law, W. Shi, G.K. Smyth, Limma powers differential expression analyses for RNA-sequencing and microarray studies, Nucleic Acids Res. 43 (2015) e47, https://doi.org/10.1093/nar/gkv007.

[17] C.J. Codden, M.T. Chin, Common and distinctive intercellular communication patterns in human obstructive and nonobstructive hypertrophic cardiomyopathy, Int. J. Mol. Sci. 23 (2022), https://doi.org/10.3390/ijms23020946.

[18] M. Chaffin, I. Papangeli, B. Simonson, A.D. Akkad, M.C. Hill, A. Arduini, S.J. Fleming, M. Melanson, S. Hayat, M. Kost-Alimova, O. Atwa, J. Ye, K.C. Bedi, M. Nahrendorf, V.K. Kaushik, C.M. Stegmann, K.B. Margulies, N.R. Tucker, P.T. Ellinor, Single-nucleus profiling of human dilated and hypertrophic cardiomyopathy, Nature 608 (2022) 174–180, https://doi.org/10.1038/s41586-022-04817-8.

[19] X. Hua, Y.Y. Wang, P. Jia, Q. Xiong, Y. Hu, Y. Chang, S. Lai, Y. Xu, Z. Zhao, J. Song, Multi-level transcriptome sequencing identifies COL1A1 as a candidate marker in human heart failure progression, BMC Med. 18 (2020) 1–16, https://doi.org/10.1186/s12916-019-1469-4.

[20] B. Jassal, L. Matthews, G. Viteri, C. Gong, P. Lorente, A. Fabregat, K. Sidiropoulos, J. Cook, M. Gillespie, R. Haw, F. Loney, B. May, M. Milacic, K. Rothfels, C. Sevilla, V. Shamovsky, S. Shorser, T. Varusai, J. Weiser, G. Wu, L. Stein, H. Hermjakob, P. D'Eustachio, The reactome pathway knowledgebase, Nucleic Acids Res. 48 (2020) D498–D503, https://doi.org/10.1093/nar/gkz1031.

[21] R. Gaujoux, C. Seoighe, A flexible R package for nonnegative matrix factorization, BMC Bioinf. 11 (2010), https://doi.org/10.1186/1471-2105-11-367.

[22] A. Subramanian, P. Tamayo, V.K. Mootha, S. Mukherjee, B.L. Ebert, M.A. Gillette, A. Paulovich, S.L. Pomeroy, T.R. Golub, E.S. Lander, J.P. Mesirov, Gene set enrichment analysis: a knowledge-based approach for interpreting genome-wide expression profiles, Proc. Natl. Acad. Sci. USA 102 (2005) 15545–15550, https://doi.org/10.1073/pnas.0506580102.

[23] M. Kanehisa, S. Goto, KEGG: kyoto encyclopedia of genes and genomes, Nucleic Acids Res. 28 (2000) 27–30, https://doi.org/10.1093/nar/28.1.27.

[24] T. Wu, E. Hu, S. Xu, M. Chen, P. Guo, Z. Dai, T. Feng, L. Zhou, W. Tang, L. Zhan, X. Fu, S. Liu, X. Bo, G. Yu, clusterProfiler 4.0: a universal enrichment tool for interpreting omics data, Innovation 2 (2021) 100141, https://doi.org/10.1016/j.xinn.2021.100141.

[25] P. Langfelder, S. Horvath, WGCNA: an R package for weighted correlation network analysis, BMC Bioinf. 9 (2008), https://doi.org/10.1186/1471-2105-9-559.

[26] J.R. Conway, A. Lex, N. Gehlenborg, UpSetR: an R package for the visualization of intersecting sets and their properties, Bioinformatics 33 (2017) 2938–2940, https://doi.org/10.1093/bioinformatics/btx364.

[27] X. Robin, N. Turck, A. Hainard, N. Tiberti, F. Lisacek, J.C. Sanchez, M. Müller, pROC: an open-source package for R and S+ to analyze and compare ROC curves, BMC Bioinf. 12 (2011) 77, https://doi.org/10.1186/1471-2105-12-77.

[28] T. Sing, O. Sander, N. Beerenwinkel, T. Lengauer, ROCR: visualizing classifier performance in R, Bioinformatics 21 (2005) 3940–3941, https://doi.org/10.1093/bioinformatics/bti623.

[29] V.S. Hahn, H. Knutsdottir, X. Luo, K. Bedi, K.B. Margulies, S.M. Haldar, M. Stolina, J. Yin, A.Y. Khakoo, J. Vaishnav, J.S. Bader, D.A. Kass, K. Sharma, Myocardial gene expression signatures in human heart failure with preserved ejection fraction, Circulation 143 (2021) 120–134, https://doi.org/10.1161/CIRCULATIONAHA.120.050498.

[30] A.M. Newman, C.L. Liu, M.R. Green, A.J. Gentles, W. Feng, Y. Xu, C.D. Hoang, M. Diehn, A.A. Alizadeh, Robust enumeration of cell subsets from tissue expression profiles, Nat. Methods 12 (2015) 453–457, https://doi.org/10.1038/nmeth.3337.

[31] E. Dann, N.C. Henderson, S.A. Teichmann, M.D. Morgan, J.C. Marioni, Differential abundance testing on single-cell data using k-nearest neighbor graphs, Nat. Biotechnol. 40 (2022) 245–253, https://doi.org/10.1038/s41587-021-01033-z.

[32] D. Sun, X. Guan, A.E. Moran, L.Y. Wu, D.Z. Qian, P. Schedin, M.S. Dai, A.V. Danilov, J.J. Alumkal, A.C. Adey, P.T. Spellman, Z. Xia, Identifying phenotype-associated subpopulations by integrating bulk and single-cell sequencing data, Nat. Biotechnol. 40 (2022) 527–538, https://doi.org/10.1038/s41587-021-01091-3.

[33] S. Jin, C.F. Guerrero-Juarez, L. Zhang, I. Chang, R. Ramos, C.H. Kuan, P. Myung, M.V. Plikus, Q. Nie, Inference and analysis of cell-cell communication using CellChat, Nat. Commun. 12 (2021) 1–20, https://doi.org/10.1038/s41467-021-21246-9.

[34] W.J. De Lange, E.T. Farrell, J.J. Hernandez, A. Stempien, C.R. Kreitzer, D.R. Jacobs, D.L. Petty, R.L. Moss, W.C. Crone, J.C. Ralphe, cMyBP-C ablation in human engineered cardiac tissue causes progressive Ca2+-handling abnormalities, J. Gen. Physiol. 155 (2023), https://doi.org/10.1085/jgp.202213204.

[35] V. Nauffal, P. Di Achille, M.D.R. Klarqvist, J.W. Cunningham, J.P. Pirruccello, L.-C. Weng, V.N. Morrill, S.H. Choi, S. Khurshid, S.F. Friedman, M. Nekoui, C. Roselli, K. Ng, A.A. Philippakis, P. Batra, P.T. Ellinor, S.A. Lubitz, Genetics of myocardial interstitial fibrosis in the human heart and association with disease, medRxiv 55 (2021), https://doi.org/10.1101/2021.11.05.21265953.
[36] G.F. Zuo, X.M. Ren, Q. Ge, J. Luo, P. Ye, F. Wang, W. Wu, Y.L. Chao, Y. Gu, X.F. Gao, Z. Ge, H. Bin Gao, Z.Y. Hu, J.J. Zhang, S.L. Chen, Activation of the PP2A catalytic subunit by ivabradine attenuates the development of diabetic cardiomyopathy, J. Mol. Cell. Cardiol. 130 (2019) 170–183, https://doi.org/10.1016/j.yjmcc.2019.04.011.
[37] D. Wang, P. Ye, C. Kong, Y. Chao, W. Yu, X. Jiang, J. Luo, Y. Gu, S.L. Chen, Mitoferrin 2 deficiency prevents mitochondrial iron overload-induced endothelial injury and alleviates atherosclerosis, Exp. Cell Res. 402 (2021) 112552, https://doi.org/10.1016/j.yexcr.2021.112552.
[38] P.M. Seferović, M. Polovina, J. Bauersachs, M. Arad, T. Ben Gal, L.H. Lund, S.B. Felix, E. Arbustini, A.L.P. Caforio, D. Farmakis, G.S. Filippatos, E. Gialafos, V. Kanjuh, G. Krljanac, G. Limongelli, A. Linhart, A.R. Lyon, R. Maksimović, D. Miličić, I. Milinković, M. Noutsias, A. Oto, Ö. Oto, S.U. Pavlović, M.F. Piepoli, A. D. Ristić, G.M.C. Rosano, H. Seggewiss, M. Ašanin, J.P. Seferović, F. Ruschitzka, J. Čelutkiene, T. Jaarsma, C. Mueller, B. Moura, L. Hill, M. Volterrani, Y. Lopatin, M. Metra, J. Backs, W. Mullens, O. Chioncel, R.A. de Boer, S. Anker, C. Rapezzi, A.J.S. Coats, C. Tschöpe, Heart failure in cardiomyopathies: a position paper from the heart failure association of the European society of cardiology, Eur. J. Heart Fail. 21 (2019) 553–576, https://doi.org/10.1002/ejhf.1461.
[39] B.J. Maron, E.J. Rowin, S.A. Casey, M.S. Link, J.R. Lesser, R.H.M. Chan, R.F. Garberich, J.E. Udelson, M.S. Maron, Hypertrophic Cardiomyopathy in Adulthood Associated with Low Cardiovascular Mortality with Contemporary Management Strategies, 2015.
[40] A. Kissopoulou, C. Trinks, A. Green, J.E. Karlsson, J. Jonasson, C. Gunnarsson, Homozygous missense MYBPC3 Pro873His mutation associated with increased risk for heart failure development in hypertrophic cardiomyopathy, ESC Heart Fail 5 (2018) 716–723, https://doi.org/10.1002/ehf2.12288.
[41] M.S. Maron, I. Olivotto, S. Betocchi, S.A. Casey, J.R. Lesser, M.A. Losi, F. Cecchi, B.J. Maron, Effect of left ventricular outflow tract obstruction on clinical outcome in hypertrophic cardiomyopathy, N. Engl. J. Med. 348 (2003) 295–303, https://doi.org/10.1056/NEJMoa021332.
[42] L.W. Liang, Y. Raita, K. Hasegawa, M.A. Fifer, M.S. Maurer, M.P. Reilly, Y.J. Shimada, Proteomics profiling reveals a distinct high-risk molecular subtype of hypertrophic cardiomyopathy, Heart (2022), https://doi.org/10.1136/heartjnl-2021-320729 heartjnl-2021-320729.
[43] U. Tayal, J.A.J. Verdonschot, M.R. Hazebroek, J. Howard, J. Gregson, S. Newsome, A. Gulati, C.J. Pua, B.P. Halliday, A.S. Lota, R.J. Buchan, N. Whiffin, L. Kanapeckaite, R. Baruah, J.W.E. Jarman, D.P. O'Regan, P.J.R. Barton, J.S. Ware, D.J. Pennell, B.P. Adriaans, S.C.A.M. Bekkers, J. Donovan, M. Frenneaux, L. T. Cooper, J.L. Januzzi, J.G.F. Cleland, S.A. Cook, R.C. Deo, S.R.B. Heymans, S.K. Prasad, Precision phenotyping of dilated cardiomyopathy using multidimensional data, J. Am. Coll. Cardiol. 79 (2022) 2219–2232, https://doi.org/10.1016/j.jacc.2022.03.375.
[44] J.A.J. Verdonschot, P. Wang, K.W.J. Derks, M.E. Adriaens, S.L.V.M. Stroeks, M.T.H.M. Henkens, A.G. Raafs, M. Sikking, B. de Koning, A. van den Wijngaard, I.P. C. Krapels, M. Nabben, H.G. Brunner, S.R.B. Heymans, Clustering of cardiac transcriptome profiles reveals unique: subgroups of dilated cardiomyopathy patients, JACC Basic Transl Sci 8 (2023) 406–418, https://doi.org/10.1016/j.jacbts.2022.10.010.
[45] S. Vakrou, Y. Liu, L. Zhu, G.V. Greenland, B. Simsek, V.B. Hebl, Y. Guan, K. Woldemichael, C.C. Talbot, M.A. Aon, R. Fukunaga, M.R. Abraham, Differences in molecular phenotype in mouse and human hypertrophic cardiomyopathy, Sci. Rep. 11 (2021) 1–19, https://doi.org/10.1038/s41598-021-89451-6.
[46] S. Bernardi, W.C. Burns, B. Toffoli, R. Pickering, M. Sakoda, D. Tsorotes, E. Grixti, E. Velkoska, L.M. Burrell, C. Johnston, M.C. Thomas, B. Fabris, C. Tikellis, Angiotensin-converting enzyme 2 regulates renal atrial natriuretic peptide through angiotensin-(1-7), Clin Sci 123 (2012) 29–37, https://doi.org/10.1042/CS20110403.
[47] J.M. Bos, V.B. Hebl, A.L. Oberg, Z. Sun, D.S. Herman, P. Teekakirikul, J.G. Seidman, C.E. Seidman, C.G. dos Remedios, J.J. Maleszewski, H.V. Schaff, J. A. Dearani, P.A. Noseworthy, P.A. Friedman, S.R. Ommen, F.V. Brozovich, M.J. Ackerman, Marked up-regulation of ACE2 in hearts of patients with obstructive hypertrophic cardiomyopathy: implications for SARS-CoV-2–mediated COVID-19, Mayo Clin. Proc. 95 (2020) 1354–1368, https://doi.org/10.1016/j.mayocp.2020.04.028.
[48] X. Liu, K. Yin, L. Chen, W. Chen, W. Li, T. Zhang, Y. Sun, M. Yuan, H. Wang, Y. Song, S. Wang, S. Hu, Z. Zhou, Lineage-specific regulatory changes in hypertrophic cardiomyopathy unraveled by single-nucleus RNA-seq and spatial transcriptomics, Cell Discov 9 (2023), https://doi.org/10.1038/s41421-022-00490-3.
[49] A. Mandawat, P. Chattranukulchai, A. Mandawat, A.J. Blood, S. Ambati, B. Hayes, W. Rehwald, H.W. Kim, J.F. Heitner, D.J. Shah, I. Klem, Progression of myocardial fibrosis in nonischemic DCM and association with mortality and heart failure outcomes, JACC Cardiovasc Imaging 14 (2021) 1338–1350, https://doi.org/10.1016/j.jcmg.2020.11.006.
[50] B. Schwartz, P. Gjini, D.M. Gopal, J.L. Fetterman, Inefficient batteries in heart failure: metabolic bottlenecks disrupting the mitochondrial ecosystem, JACC Basic Transl Sci 7 (2022) 1161–1179, https://doi.org/10.1016/j.jacbts.2022.03.017.
[51] P.G. Camici, C. Tschöpe, M.F. Di Carli, O. Rimoldi, S. Van Linthout, Coronary microvascular dysfunction in hypertrophy and heart failure, Cardiovasc. Res. 116 (2020) 806–816, https://doi.org/10.1093/cvr/cvaa023.
[52] J.G. Travers, F.A. Kamal, J. Robbins, K.E. Yutzey, B.C. Blaxall, Cardiac fibrosis: the fibroblast awakens, Circ. Res. 118 (2016) 1021–1040, https://doi.org/10.1161/CIRCRESAHA.115.306565.
[53] X. Zou, H. Ouyang, F. Lin, H. Zhang, Y. Yang, D. Pang, R. Han, X. Tang, MYBPC3 deficiency in cardiac fibroblasts drives their activation and contributes to fibrosis, Cell Death Dis. 13 (2022) 1–10, https://doi.org/10.1038/s41419-022-05403-6.
[54] Q. Meng, B. Bhandary, M.S. Bhuiyan, J. James, H. Osinska, I. Valiente-Alandi, K. Shay-Winkler, J. Gulick, J.D. Molkentin, B.C. Blaxall, J. Robbins, Myofibroblast-specific TGFβ receptor II signaling in the fibrotic response to cardiac myosin binding protein C-induced cardiomyopathy, Circ. Res. 123 (2018) 1285–1297, https://doi.org/10.1161/CIRCRESAHA.118.313089.
[55] J.J.V. McMurray, M. Packer, A.S. Desai, J. Gong, M.P. Lefkowitz, A.R. Rizkala, J.L. Rouleau, V.C. Shi, S.D. Solomon, K. Swedberg, M.R. Zile, Angiotensin–neprilysin inhibition versus enalapril in heart failure, N. Engl. J. Med. 371 (2014) 993–1004, https://doi.org/10.1056/NEJMoa1409077.
[56] Y. Nakagawa, T. Nishikimi, K. Kuwahara, Atrial and brain natriuretic peptides: hormones secreted from the heart, Peptides (N.Y.) 111 (2019) 18–25, https://doi.org/10.1016/j.peptides.2018.05.012.
[57] W. Yan, F. Wu, J. Morser, Q. Wu, Corin, a transmembrane cardiac serine protease, acts as a pro-atrial natriuretic peptide-converting enzyme, Proc Natl Acad Sci U S A 97 (2000) 8525–8529, https://doi.org/10.1073/pnas.150149097.
[58] N. Dong, S. Chen, J. Yang, L. He, P. Liu, D. Zheng, L. Li, Y. Zhou, C. Ruan, E. Plow, Q. Wu, Plasma Soluble Corin in patients with heart failure, Circ Heart Fail 3 (2010) 207–211, https://doi.org/10.1161/CIRCHEARTFAILURE.109.903849.
[59] U.N. Ibebuogu, I.P. Gladysheva, A.K. Houng, G.L. Reed, Decompensated heart failure is associated with reduced corin levels and decreased cleavage of pro-atrial natriuretic peptide, Circ Heart Fail 4 (2011) 114–120, https://doi.org/10.1161/CIRCHEARTFAILURE.109.895581.
[60] R. Tripathi, D. Wang, R. Sullivan, T.H.M. Fan, I.P. Gladysheva, G.L. Reed, Depressed corin levels indicate early systolic dysfunction before increases of atrial natriuretic peptide/B-type natriuretic peptide and heart failure development, Hypertension 67 (2016) 362–367, https://doi.org/10.1161/HYPERTENSIONAHA.115.06300.
[61] X. Zhang, X. Gu, Y. Zhang, N. Dong, Q. Wu, Corin: a key mediator in sodium homeostasis, vascular remodeling, and heart failure, Biology 11 (2022) 1–15, https://doi.org/10.3390/biology11050717.
[62] A.G. Semenov, N.N. Tamm, K.R. Seferian, A.B. Postnikov, N.S. Karpova, D.V. Serebryanaya, E.V. Koshkina, M.I. Krasnoselsky, A.G. Katrukha, Processing of pro-B-type natriuretic peptide: furin and corin as candidate convertases, Clin. Chem. 56 (2010) 1166–1176, https://doi.org/10.1373/clinchem.2010.143883.
[63] I.P. Gladysheva, D. Wang, R.A. McNamee, A.K. Houng, A.A. Mohamad, T.M. Fan, G.L. Reed, Corin overexpression improves cardiac function, heart failure, and survival in mice with dilated cardiomyopathy, Hypertension 61 (2013) 327–332, https://doi.org/10.1161/HYPERTENSIONAHA.112.193631.
[64] R. Tripathi, R.D. Sullivan, T.H.M. Fan, A.K. Houng, R.M. Mehta, G.L. Reed, I.P. Gladysheva, Cardiac-specific overexpression of catalytically inactive corin reduces edema, contractile dysfunction, and death in mice with dilated cardiomyopathy, Int. J. Mol. Sci. 21 (2020), https://doi.org/10.3390/ijms21010203.